NANO LETTERS

2007
Vol. 7, No. 9
2795−2799

Transcending Binary Logic by Gating Three Coupled Quantum Dots

Michael Klein,[‡] S. Rogge,[§] F. Remacle,[†,‡,||] and R. D. Levine*[,‡,⊥]

The Fritz Haber Research Center for Molecular Dynamics, The Hebrew University of Jerusalem, Jerusalem 91904, Israel, Kavli Institute of Nanoscience, Delft University of Technology, Lorentzweg 1, 2628 CJ Delft, The Netherlands, Département de Chimie, B6c, Université de Liège, B4000 Liège, Belgium, and Department of Chemistry and Biochemistry, The University of California Los Angeles, Los Angeles, California 90095-1569

Received June 8, 2007; Revised Manuscript Received August 7, 2007

ABSTRACT

Physical considerations supported by numerical solution of the quantum dynamics including electron repulsion show that three weakly coupled quantum dots can robustly execute a complete set of logic gates for computing using three valued inputs and outputs. Input is coded as gating (up, unchanged, or down) of the terminal dots. A nanosecond time scale switching of the gate voltage requires careful numerical propagation of the dynamics. Readout is the charge (0, 1, or 2 electrons) on the central dot.

The correspondence between switching networks and a Boolean algebra of two elements 0 and 1 goes back to Shannon (1938). Bistable devices are straightforward to construct, and their operation is so robust that computing using switches has survived several decades of technological developments. We however do not know of a reason of principle why two-valued variables must be used. One direction of applications where multivalued variables are common is coding.[1,2] The Morse code that uses three different symbols is probably the best known, and natural languages use many more than three distinct symbols. The more there are distinct symbols, the shorter are the code words. Thus the number nine is denoted as 9 in the usual decimal notation, as 100 in a base three, and as 1001 in base two. The complementary aspect is that the larger the radix, the more states need to be physically distinguishable. Assume that the cost is proportional to the need for storage (= length of word $\propto$ 1/log(radix)) and to the number of states (= radix) of the multivalued device that must be resolved. Then, if the radix is taken to be a continuous variable, the natural number *e* is the optimal choice. This motivates three-valued logic functions as a best practical choice.[3]

In this letter, we provide a physical realization of a complete set of gates. Each gate accepts three-valued inputs and has a three-valued output. Complete set means that a logic circuit for any other function can be constructed using only gates of the set. It turns out that it is enough to consider gates that accept as input just one or two (three-valued) variables. The saving aspect is that, while there are $3^9 = 19\,683$ different three-valued functions of two three-valued variables, we need only two such functions in the complete set.[3] The complete set is not unique. In the more familiar switching case, there are 2^4 functions of two variables and a complete set using only one such function (e.g., NOT−AND) is possible.[4] Other choices of a complete set consisting of two or even three functions are familiar and can lead to simpler circuits for evaluation of the other functions.

The complete set of gates is implemented here on an array of three coupled metallic quantum dots (QD), see Scheme 1. To establish the operation, we consider the limit where the orbital level spacing of the dot, δ, is much smaller than the Coulomb energy of adding an electron, *I*. Because we use metallic dots, they will have one valence electron in their ground state and each can accommodate one or two electrons (of opposite spins). The occupancy of the valence orbital (usually on the central dot) is the readout of our logic schemes.

Species that span a wide range of sizes, from molecular to micro (i.e., molecules, colloidal QD, lithographic QD, metallic SET, etc.) that can be multicharged are known, see for example refs 5−19. Here we will use just the valence occupancy of such a species. To reduce the Coulombic repulsion *I* between the electrons on the same dot, we use quantum dots whose charging energy is lower than that of

* Corresponding author. E-mail: rafi@fh.huji.ac.il.
[†] F.R. is Directeur de Recherches, FNRS (Belgium).
[‡] The Fritz Haber Research Center for Molecular Dynamics, The Hebrew University of Jerusalem.
[§] Kavli Institute of Nanoscience, Delft University of Technology.
[||] Département de Chimie, B6c, Université de Liège.
[⊥] Department of Chemistry and Biochemistry, The University of California Los Angeles.

10.1021/nl071376e CCC: $37.00
Published on Web 08/21/2007

Scheme 1. Schematic of the Device Consisting of a Linear Array of Three Quantum Dots, the Gates on the Two Terminal Dots, Labeled as G1 and 2 and the Single Electron Transistor (SET) Readout of the Charge on the Central Dot[a]

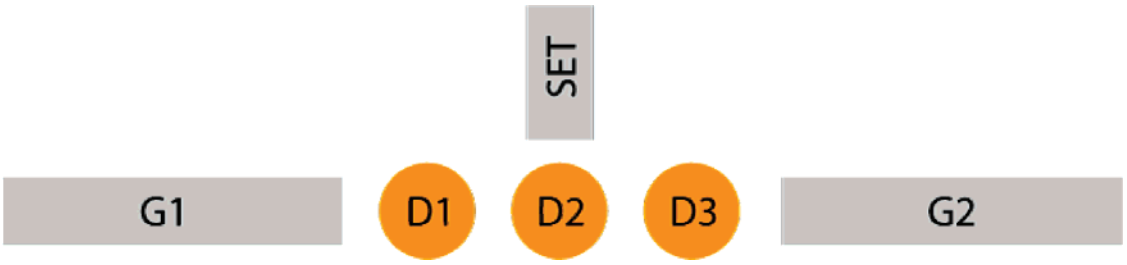

[a] The input is the change of a gate voltage (down, no change, up). The output is the charge on the middle dot (0,1,2) coded as (−1,0,1).

atoms, $I \gg \delta$.[18,20−22] This is the case for a dot where the Fermi wavelength is much shorter than the dot size. However, there is a limit on how large the dots can be because we need the charging energy to be distinctly resolvable from the next higher state in the addition spectrum compared to the thermal energy. So a compromise is required if we are to offer a design that can operate at a finite temperature. Furthermore, the coupling to the environment needs to be sufficiently weak so the number of electrons on the device is a good quantum number.

We use an array of three quantum dots as, for example, in refs 8,23−26. We need to be able to separately gate the two end dots because, for the gate that evaluates a function of two independent variables, the two inputs are applied as gate voltages on the dots on the left and on the right, Scheme 1. The three values of the input are gate voltage lowered, unchanged, or raised. The dots are weakly exchange coupled and as discussed in the next paragraph. It is the response to the gating induced by this coupling that serves to perform the function evaluation. Scheme 1 shows a layout of the array, the input gates, and a readout on the central dot. Note that the energy scale of such a device is not set by the dimension of the leads but rather that of the molecular/atomic system and its coupling to the environment.[5,17] Recent experimental progress on atomic-scale contacts[27,28] is impressive and will allow for more evolved nanostructures in the near future. The device that we describe, consisting of three dots can, by itself and without concatenation to other gates, evaluate the two functions of two variables, called below the MIN and the MAX, that together with unary functions provide a complete set.[29−31] That a single device can do the entire function evaluation is an essential progress.

The physics of the device is that of a row of three dots of similar size that are weakly exchange coupled. The charging energy I of a dot is taken to be larger than the coupling, β, where β is the transfer integral between neighboring dots. The two end dots are gated. When the charging energy is not small, $I \gg \delta$, we can use a simple model of just one valence orbital per dot and the gating alters the energy, α, of this orbital. The quantitative description is provided by a Hubbard-like Hamiltonian, given explicitly in eq 1 below. The only difference form the standard usage of such a Hamiltonian, e.g., in ref 32, is that the Hamiltonian in eq 1 is time dependent because the gate voltages are switched on and off, as required to code the inputs. The quantum

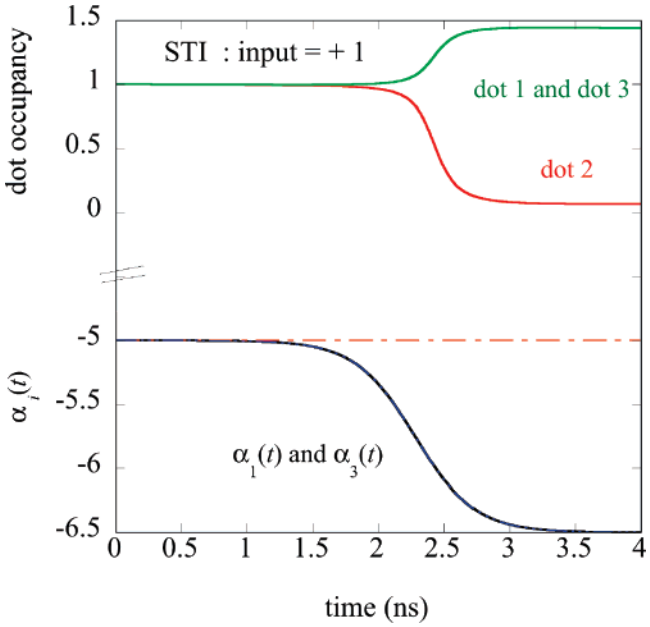

Figure 1. Occupancy of the three dots, ($\mathbf{c}^{\mathrm{T}}\hat{\mathbf{E}}_{i,i}\mathbf{c}$, i = 1,2,3, see Supporting Information), as computed by a solution of the time-dependent Schroedinger equation for nanosecond switching of the gate potentials on both of the two end dots. The total number of valence electrons on the dot array is equal to 3. The time constant of the switching is 0.45 ns. This simulation mimics the operation of the STI gate of Table 1 for the input +1. Input −1 corresponds to an increase of the voltage on dots 1 and 3 (see Table 1). The output for input 0 is equal to 0 (1 electron on dot 2) and can be read from the short time occupancy of dot 2. For each value of the output, we define a range of acceptance, e.g., we read occupancy as 2 (logic value 1) when the actual occupancy is above 1.6. In eq 1, I = 0.5 eV and β = 0.08 eV. The initial values of the valence orbitals are $\alpha_1 = \alpha_2 = \alpha_3 = -5.0$ eV.

dynamics is simulated by an exact numerical procedure as discussed further below and in the Supporting Information. Next, we provide a qualitative discussion of the gate action.

Say we have three active electrons on the device. Consider a state where the charge is uniformly distributed on the three dots. Because of the exchange coupling β, in principle, this state is not necessarily stationary. But the dots are comparable in size and so have similar, differences of the order of β, orbital energies and a uniform distribution can be maintained as verified by the exact computations shown in Figure 1. Now we alter the gate voltage on the two end dots as also shown in Figure 1. As the orbital energy of dots 1 and 3 is lowered by the gating, there comes a point where it is low

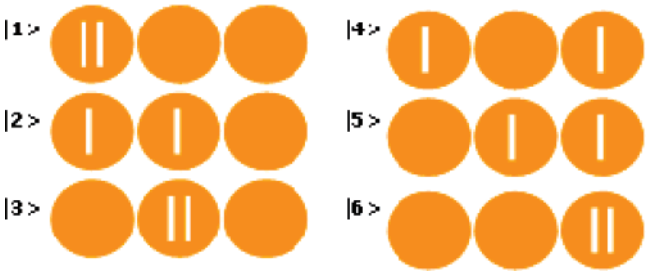

Figure 2. Complete set of basis states for a singlet state of two electrons on three dots with one orbital per dot, designated as $|i\rangle$, $i = 1,..,6$. Constructed and numbered as discussed in ref 35. These states are all eigenstates of the occupation operators $E_{i,i}$ and so diagonalize the Hamiltonian, eq 1, for the special case of uncoupled dots, $\beta = 0$. Three states have the middle dot empty, two states have one electron on the middle dot. For one state, the middle dot is doubly occupied.

enough that it becomes energetically advantageous for the charge to depart from dot 2 and to be shared by dots 1 and 3. The switch occurs when the gain in energy by the gating compensates for the repulsive charging energy I that occurs when two electrons are on the same dot. To enable such a point to be possible and to ensure that the resulting charge reorganization is stable, it is necessary that $I \gg \beta \approx \Delta\alpha$, where $\Delta\alpha$ is the difference in orbital energies. (Unless $I \gg \Delta\alpha$, the Coulomb blockade can be compensated by the difference in orbital energies of adjacent dots, as can occur in arrays of disordered dots[33]). After the gating is over, neighboring dots are not resonant and the superexchange coupling between the two terminal dots, $\approx \beta^2/I$, is very weak, so one can wait and read that the central dot is empty of charge, see Figure 1. Gating that compensates for charging energy can therefore be used to control the charge on the central dot. The quantitative theory, Figure 1, serves only to validate this simple picture.

For evaluating a function of two variables, we first gate one end dot and then gate the other end as shown in Figure 3 below. So the discussion in the paragraph above of evaluating a function of one variable still applies but in two stages.

The quantum dynamics is computed in the basis set provided by the representation of the unitary group,[34−36] and we have employed it previously in studies of arrays of few coupled dots.[33,37] The basis states assign a definite number of electrons to each dot. For implementing the ternary gates, we use arrays of two, three, or four electrons in the lowest spin state. For three dots and three valence electrons in a doublet state, there are eight basis states. Both for the two- and the four-electron array, there are six singlet basis states. In Figure 2, we show dot occupancy of the six singlet basis states of an array with a total of two electrons. The basis states do not fully diagonalize the Hubbard Hamiltonian but do have the very attractive feature that they diagonalize the bielectronic Coulomb repulsion, which is the otherwise hard to handle term. The basis states do not diagonalize the weak exchange coupling between the dots. It is therefore necessary to numerically diagonalize the Hamiltonian. A singlet eigenstate of the Hubbard Hamiltonian for three dots and

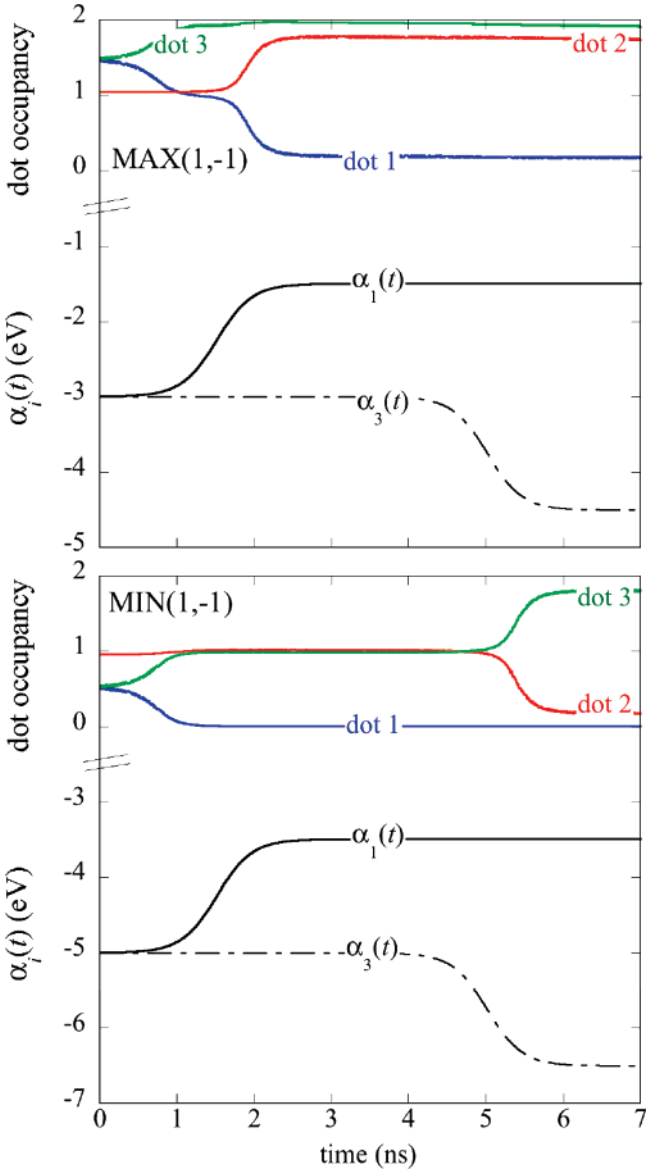

Figure 3. Time evolution of the dot occupancies and of their energies, for the implementation of a MAX gate (top) and a MIN gate (bottom). Results are for the input (1,−1) or, in physical terms, increase α_1 then decrease α_3 as shown in the plot. For the MIN gate and the MAX gates, the initial values of α_1 and α_3 are 5 eV, $I = 0.5$ eV, and $\beta = 0.08$ eV. For the MAX gate, α_2 is equal to −4.7 eV, and there are a total of four valence electrons in the dot array, while for the MIN gate, α_2 is equal to −5.3 eV and there are two valence electrons. In both case, the $\Delta\alpha$ resulting from the lowering or the raising of the valence orbital energy by the gate voltage is equal to 1.5 eV.

two electrons is then exactly expressed as a linear combination of the six zero-order basis states $|\psi_\alpha\rangle = \sum_{i=1}^{6} c_{\alpha i}|i\rangle$.

Explicitly, the many-electron Hamiltonian for the device is

$$\hat{H} = \sum_{i=1}^{3} \alpha_i(t)\hat{E}_{i,i} + \beta \sum_{i,j,i\neq j}^{3} \hat{E}_{i,j} + \frac{1}{2} I \sum_{i=1}^{3} \hat{E}_{i,i}(\hat{E}_{i,i} - 1) \quad (1)$$

The Hamiltonian is time dependent because the gating changes the energies of the dots. $\hat{E}_{i,i}$ is the operator for the

Table 1. Three Unary Gates (One Input, Physically Applied as a Gate Voltage on the Two Terminal Dots Leading to a Change in Their Orbital Energy)[a]

input	Δα	STI	PTI	NTI	FD	RD
−1	up	1	1	1	0	−1
0	no change	0	1	−1	0	0
1	down	−1	−1	−1	1	0

[a] See Figure 1 for the time evolution of the charge of all three dots for the STI gate with input + 1 and the graphical abstract for the long-time occupancy of dot 2 for the STI, PTI, and NTI gates with a nanosecond time scale switching). The single unary gates known as forward and reverse diodes, (FD and RD), can be generated as the PTI and NTI gates but with reading the output on an end dot. The five unary gates shown together with the two binary gates shown in Table 2 suffice to provide a complete set.[29,30] The parameters used to implement the PTI gate are $\alpha_1 = \alpha_3 = -5.0$, $\alpha_2 = -5.3$ eV and a total of four electrons on the array while for the NTI gate, $\alpha_1 = \alpha_3 = -5.0$, $\alpha_2 = -4.7$ eV and there are two electrons on the array. The parameters used for implementing the STI are given in the legend of Figure 1.

Table 2. MIN (upper) and MAX (lower) Binary Gates for Ternary Logic[a]

	MIN		
input	−1	0	1
−1	−1	−1	−1
0	−1	0	0
1	−1	0	1
	MAX		
input	−1	0	1
−1	−1	0	1
0	0	0	1
1	1	1	1

[a] The top row and the left column show the two inputs where the numbers indicate the direction of change of the gate voltage of the dots on the right and the left; this is opposite to the encoding of the inputs used for the unary gates shown in Table 1.

occupancy of the ith dot, and $\hat{E}_{i,j}$ is the transfer operator from dot i to dot j. The energy of an electron in the valence orbital of dot i, $\alpha_i(t)$, is time dependent because the input is provided as a variation of the gate voltage on a dot. It can stay at zero or it can be increased or decreased. For simplicity, we take the exchange integral β and the charging energy I to be equal for the three dots, but this is not required by the formalism. As discussed above, we take $\beta \ll I$ so that it requires a gating to move the charge to any significant extent.

The reading of the output is the determination of the occupancy of the central dot. The proper action of a logic circuit requires therefore that the gating of the end dots drives the state of the system toward a definite occupancy that is dictated by the input. The more it is able to do so, the more robust is the reading of the output.

The gate voltages are switched on or off on a realistic nanosecond time scale, and the response of the system is determined by solving the time-dependent Schroedinger equation with the ground electronic state of the not gated array as the initial state. Details of the computations are provided as Supporting Information.

Table 1 is the truth table for a choice of (five out of a total of 27) unary gates (= gates that compute a function of one variable). Simple ternary inverter (STI), positive ternary inverter (PTI), negative ternary inverter (NTI), and forward and reverse diodes (FD and RD) that with two binary gates form a complete set.[29−31] For the unary gates, the input is

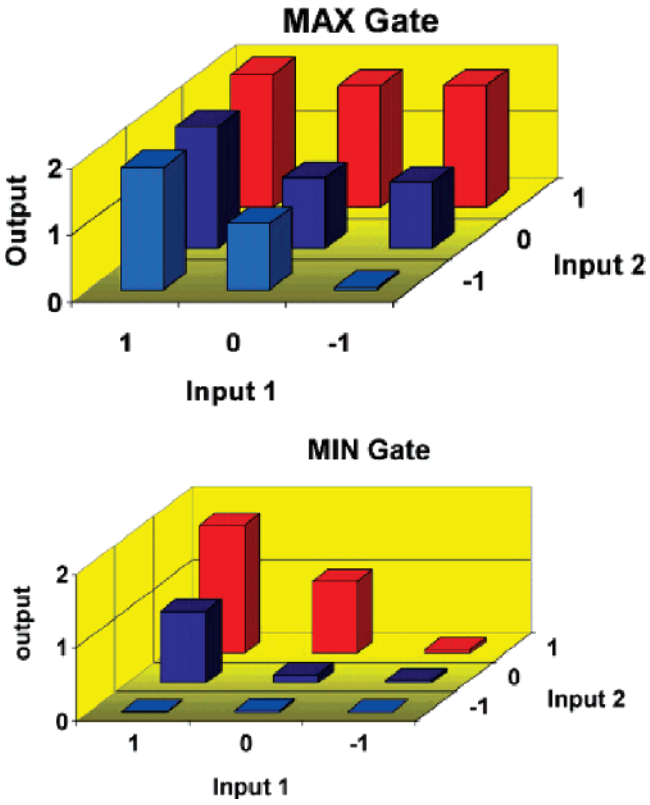

Figure 4. Long-time occupancy of the middle dot (coded as −1, 0, or 1) as determined by a solution of the time-dependent Schroedinger equation for nanosecond switching of the gate potentials on the two end dots computed for a MAX (top) and MIN (bottom) gate. The parameters used are those reported in Figure 3. The two ternary inputs, x and y, are encoded in gating dot 1 and dot 3 successively in time with a nanosecond variation. The change in the α's induced by the gates are 1.5 eV up or down. Figure 3 shows the output for the inputs (1,−1).

applied as a simultaneous variation of the gate voltages on the two end dots. An example, a STI gate, is shown in Figure 1. For the inverter gates, we read the output as the long-time occupancy of the middle dot coded as −1, 0, 1, meaning no charge, one, or two electrons. For the diode gates, we read on an end dot. It is not going to be possible to hit the desired values of the charge (i.e., 0, 1, or 2) exactly. As shown in Figures 1 and 3, it is possible to reach values that rather clearly can be assigned to one of the three values. To avoid ambiguity, we assign the bins 0 to 0.4, 0.8 to 1.2, and 1.6 to 2 as the values of the three readouts, and it is possible to choose realistic values for the physical parameters such that the readouts fall comfortably within the indicated ranges. Specifically for all gates discussed herein, the initial values of $I = 0.5$ eV and $\beta = 0.08$ eV will work, with the change in the valence orbitals α_i, $i = 1$ and 3 (due to gating) of 1.5 eV. Dot 2 is not gated and therefore α_2 remains unchanged.

In Figure 3, we show the time evolution of the dot occupancies for the case of a ternary input $x = 1$ and $y = -1$ for both the MAX (top) and the MIN (bottom) gate. Max (1,−1) is 1, coded into a final occupancy of dot 2 by two electrons (top), while MIN (1,−1) is −1, coded into a final occupancy of 0 electrons on dot 2. The two ternary inputs

are encoded as a gating voltage, raising the valence orbital of dot 1 or dot 3 by 1.5 eV (+1) or lowering by 1.5 eV (−1). The *x* input corresponds to a gate voltage applied to dot 1, while the *y* input corresponds to a gate voltage applied to dot 3 and is delayed with respect to the voltage applied to dot 1. One can see from the figure that, for this more elaborate dynamics also, the reading of the output as the occupancy of dot 2 falls comfortably within the indicated range.

Figure 4 summarizes the computed outputs for all nine possible ternary inputs (*x*,*y*) for the MAX (top) and MIN (bottom) gates. Here, too, it is very clear that the assignment of the final charge of the middle dot is definitely unambiguous.

After an evaluation, the system can be reset such that it is ready for a next computation. In principle, it is not necessary to assume that the electronic state relaxes back to the ground state before the next function evaluation. If relaxation can be arrested and because the temporal response will be different depending on which is the initial state, we can operate the device not only for evaluating a function of the inputs (what is called a combinational circuit) but also as a device that also remembers the output of the previous operation (meaning as a finite state machine[4,38,39]). Electronic population relaxation to the environment limits for how long the memory of the occupancy is maintained. In this letter, we only discussed function evaluation. Also, as discussed in the Supporting Information, because the switching of the gate voltage is done on the nanosecond time scale, care is required to guard against the numerically induced dephasing of the wave function. This means that, because of the inevitable environmental perturbations that will be present in a real experiment, the device is not ideally suited to act as a quantum computer. For this reason, we use as output only the occupancy but not the phase, what we sometimes call[40] "a quasiclassical computation".

In conclusion, a single nanodevice of three coupled metallic quantum dots with the input provided at two gates at the terminals and a single electron transistor readout of the charge of a single dot performs a complete set of ternary logic gates.

Acknowledgment. Critical resources for this research were provided by the MOLDYNLOGIC STREP FET-Open EC project (www.moldynlo.ulg.ac.be). Exchange funds were provided by the EC NoE FAME (www.famenoe.org).

Supporting Information Available: Discussion of the quantum dynamics simulated by an exact numerical procedure; details of the computations.[41] This material is available free of charge via the Internet at http://pubs.acs.org.

References

(1) Roman, S. *Coding and Information Theory*; Springer-Verlag: New York, 1992.
(2) Hamming, R. W. *Coding and Information Theory*; Prentice Hall: Upper Saddle River, NJ, 1986.
(3) Hurst, S. L. *IEEE Trans. Comput.* **1984**, *C-33*, 1160−1179.
(4) Kohavi, Z. *Switching and Finite Automata Theory*; Tata McGraw-Hill: New Delhi, 1999.
(5) Sellier, H.; Lansbergen, G. P.; Caro, J.; Rogge, S.; Collaert, N.; Ferain, I.; Jurczak, M.; Biesemans, S. *Phys. Rev. Lett.* **2006**, *97*, 206805.
(6) Sellier, H.; Lansbergen, G. P.; Caro, J.; Rogge, S.; Collaerts, N.; Ferain, I.; Jurczak, M.; Biesemans, S. *Appl. Phys. Lett.* **2007**, *90*, 073502.
(7) Katz, E.; Lioubashevski, O.; Willner, I. *Chem. Commun.* **2006**, *10*, 1109−1111.
(8) Gaudreau, L.; Studenikin, S. A.; Sachrajda, A. S.; Zawadzki, P.; Kam, A.; Lapointe, J.; Korkusinski, M.; Hawrylak, P. *Phys. Rev. Lett.* **2006**, *97*, 036807.
(9) Weiss, D. N.; Brokmann, X.; Calvet, L. E.; Kastner, M. A.; Bawendi, M. G. *Appl. Phys. Lett.* **2006**, *88*, 143507.
(10) Fujiwara, A.; Inokawa, H.; Yamazaki, K.; Namatsu, H.; Takahashi, Y.; Zimmerman, N. M.; Martin, S. B. *Appl. Phys. Lett.* **2006**, *88*, 053121.
(11) Ono, Y.; Fujiwara, A.; Nishiguchi, K.; Inokawa, H.; Takahashi, Y. *J. Appl. Phys.* **2005**, *97*, 031101−031119.
(12) Mason, N.; Biercuk, M. J.; Marcus, C. M. *Science* **2004**, *303*, 655−658.
(13) Bjork, M. T.; Thelander, C.; Hansen, A. E.; Jensen, L. E.; Larsson, M. W.; Wallenberg, L. R.; Samuelson, L. *Nano Lett.* **2004**, *4*, 1621−1625.
(14) De Franceschi, S.; van Dam, J. A.; Bakkers, E.; Feiner, L. F.; Gurevich, L.; Kouwenhoven, L. P. *Appl. Phys. Lett.* **2003**, *83*, 344−346.
(15) Quinn, B. M.; Liljeroth, P.; Ruiz, V.; Laaksonen, T.; Kontturi, K. *J. Am. Chem. Soc.* **2003**, *125*, 6644−6645.
(16) Takahashi, Y.; Ono, Y.; Fujiwara, A.; Inokawa, H. *Physica E* **2003**, *19*, 95−101.
(17) Park, J.; Pasupathy, A. N.; Goldsmith, J. I.; Chang, C.; Yaish, Y.; Petta, J. R.; Rinkoski, M.; Sethna, J. P.; Abrun, H. D.; McEuen, P. L.; Ralph, D. C. *Nature* **2002**, *417*, 722−725.
(18) Kouwenhoven, L. P.; Austing, D. G.; Tarucha, S. *Rep. Prog. Phys.* **2001**, *64*, 701−736.
(19) Augke, R.; Eberhardt, W.; Strahle, S.; Prins, F. E.; Kern, D. P. *Microelectron. Eng.* **1999**, *46*, 141−144.
(20) Ashoori, R. C. *Nature* **1996**, *379*, 413−419.
(21) Kastner, M. A. *Phys. Today* **1993**, *46*, 24−31.
(22) Averin, D. V.; Korotkov, A. N.; Likharev, K. K. *Phys. Rev. B* **1991**, *44*, 6199−6211.
(23) Waugh, F. R.; Berry, M. J.; Crouch, C. H.; Livermore, C.; Mar, D. J.; Westervelt, R. M.; Campman, K. L.; Gossard, A. C. *Phys. Rev. B* **1996**, *53*, 1413−1420.
(24) Waugh, F. R.; Berry, M. J.; Mar, D. J.; Westervelt, R. M.; Campman, K. L.; Gossard, A. C. *Phys. Rev. Lett.* **1995**, *75*, 705−708.
(25) Bajec, I. L.; Zimic, N.; Mraz, M. *Nanotechnology* **2006**, *17*, 1937−1942.
(26) Xu, K.; Green, J. E.; Heath, J. R.; Remacle, F.; Levine, R. D. *J. Phys. Chem. C* **2007**, *111*, jp071353o.
(27) Ruess, F. J.; Oberbeck, L.; Simmons, M. Y.; Goh, K. E. J.; Hamilton, A. R.; Hallam, T.; Schofield, S. R.; Curson, N. J.; Clark, R. G. *Nano Lett.* **2004**, *4*, 1969−1973.
(28) Ruess, F. J.; Pok, W.; Goh, K. E. J.; Hamilton, A. R.; Simmons, M. Y. *Phys. Rev. B* **2007**, *75*, 121303(R).
(29) Yoeli, M.; Rosenfeld, G. *IEEE Trans. Elect. Comput.* **1965**, *EC-14*, 19−29.
(30) Halpern, I.; Yoeli, M. *Proc. IEE* **1968**, *115*, 1385−1388.
(31) Bajec, I. L.; Zimic, N.; Mraz, M. *Microelectron. Eng.* **2006**, *83*, 1826−1829.
(32) Chen, G. L.; Klimeck, G.; Datta, S.; Chen, G. H.; Goddard, W. A. *Phys. Rev. B* **1994**, *50*, 8035−8038.
(33) Remacle, F.; Levine, R. D. *J. Am. Chem. Soc.* **2000**, *122*, 4084−4091.
(34) Hinze, J. *The Unitary Group Approach for the Evaluation of Electronic Energy Matrix Elements*; Springer: Berlin, 1981; Vol. 22, Lecture Notes in Chemistry.
(35) Paldus, J. *J. Chem. Phys.* **1974**, *61*, 5321−5330.
(36) Shavitt, I. *Int. J. Quantum Chem.* **1977**, *S11*, 131−148.
(37) Remacle, F.; Levine, R. D. *ChemPhysChem* **2001**, *2*, 20−36.
(38) Remacle, F.; Levine, R. D. *J. Chem. Phys.* **2001**, *114*, 10239−10246.
(39) Steinitz, D.; Remacle, F.; Levine, R. D. *ChemPhysChem* **2002**, *3*, 43−51.
(40) Remacle, F.; Levine, R. D. *Proc. Natl. Acad. Sci. U.S.A.* **2004**, *101*, 12091−12095.
(41) Remacle, F.; Levine, R. D. *J. Chem. Phys.* **1999**, *110*, 5089−5099.

NL071376E